Exploring the Efficacy of Sawdust Ash as a Mineral Filler Substitute for the Production of Asphalt Mixtures

Mayank Sukhija[1*]; Aliaa F. Al-ani[2]; Hussein K. Mohammad[3]; Amjad Albayati[4]; and Yu Wang[5]

[1]*School of Civil and Construction Engineering, Oregon State University, OR, 97331, USA; sukhijam@oregonstate.edu, *Corresponding author*

[2]*Department of Civil Engineering, University of Baghdad, Baghdad 10071, Iraq; Aliaa.faleh@coeng.uobaghdad.edu.iq*

[3]*Ministry of Higher Education and Scientific Research, Baghdad 10072, Iraq; renosprt@gmail.com*

[4]*Department of Civil Engineering, University of Baghdad, Baghdad 10071, Iraq; a.khalil@uobaghdad.edu.iq*

[5]*School of Science, Engineering & Environment, University of Salford, Manchester M5 4WT, UK; Y.Wang@salford.ac.uk*

Abstract: Many waste materials can be repurposed effectively within asphalt concrete to enhance the performance and sustainability of pavement. One of these waste materials is sawdust ash (SDA). This study explores the beneficial use of SDA as a substitute for limestone dust (LD) mineral filler in asphalt concrete. The replacement rate was 0%, 15%, 30%, 45%, and 60% by weight of total mineral filler. Scanning electron microscopy (SEM) was employed to assess the surface morphology of Sawdust (SD), SDA, and LD. In addition, a series of tests, including Marshall stability and flow, indirect tensile strength, moisture susceptibility, and repeated uniaxial loading tests, were conducted to examine the performance characteristics of asphalt mixtures of different SDA content. As per Marshall mix design, a slightly higher binder content was required for the preparation of SDA mixes. The results reveal that the asphalt mixtures prepared using SDA attain a tensile strength ratio (TSR) greater than the critical threshold, i.e., 80%, indicating the feasibility of SDA against moisture-induced damage. The highest TSR value of 87% was obtained using 45% SDA as a replacement for LD. Compared to 0% SDA, there is a reduction of 12.08% in permanent deformation for asphalt mixtures produced with 60% SDA. Also, as the SDA content increases, there is a slight improvement in the resilient modulus values, with a peak improvement of 3% at 60% SDA. In addition, the cost of producing SDA mixes was relatively lower than the control mixes, indicating the cost-

effectiveness of using SDA. Overall, the study found that SDA is a promising material that can improve the performance and durability of asphalt concrete at lower production costs.

Keywords: Sawdust ash, Asphalt concrete, Moisture damage, Resilient modulus, Permanent deformation

1. Introduction

Asphalt surfacing, commonly known as asphalt concrete, has been widely adopted in road construction throughout the globe. Production of asphalt concrete requires large amounts of non-renewable materials such as aggregate and mineral filler, consuming substantial natural resources. As a result, there is growing interest in developing sustainable asphalt concrete, facing increasing natural resource shortages and environmental pollution [1]. One effort to achieve sustainability in asphalt concrete is to use sustainable mineral fillers. Sustainable mineral fillers are materials produced from waste streams or renewable resources, which can be alternatives to traditional mineral fillers [2]. Some examples of sustainable mineral fillers that have been investigated include sawdust ash, fly ash, bagasse ash, brick dust, ceramic waste, red mud, coal mine waste, glass powder, kota-stone dust, cement concrete dust, etc [3, 4]. Mineral fillers are fine powders less than 75 μm (No. 200) in size. They are added into asphalt concrete with a typical content ranging from 2 to 12 percent by weight of the total mixture [5-7]. The main purpose of mineral fillers is to fill the voids between the aggregate particles, which helps to improve the packing density of the mixture and enhance the stability, strength, and durability of the asphalt concrete mixtures [8]. Using sustainable mineral fillers in asphalt concrete can potentially reduce the environmental impact of road construction while maintaining or potentially enhancing the performance of asphalt pavements [9-11]. As the type and content of the mineral filler play an important role in the performance of the asphalt concrete mixtures, material selection becomes crucial [3].

Around the globe, sawdust ash (SDA) is one of the abundant waste materials generated during the combustion of sawdust or other wood products, typically generated in biomass power plants or wood-processing industries. It is a fine powder that can be collected from the exhaust gases of wood-fired boilers or furnaces [12]. Reusing SDA helps minimize waste generation, reduce the cost of waste management, and promote sustainable engineering practices. SDA has a high silica and low carbon content, which makes it an effective alternative for the mineral fillers used in asphalt concrete. A study conducted by Osuya and Mohammed [13] found that including SDA in asphalt concrete reduced the rutting deformation of the pavement due to the increased stiffness of the mixture. Another study by Karati et al. [14] on the moisture susceptibility of asphalt mixtures has found that asphalt mixtures comprising SDA have less potential for moisture damage [14]. Fayissa et al. [15] evaluated the effects of SDA on the mechanical and rheological properties of asphalt concrete. They reported that SDA in asphalt concrete can improve mechanical properties, including the Marshall stability, flow value, and indirect tensile strength. Additionally, the use of SDA improves the high-temperature performance of asphalt concrete.

SDA content plays a key role in influencing the performance of asphalt concrete. As per Abbas et al. [16], 60% SDA content can be used as a substitute for ordinary portland cement (OPC) to achieve the adequate performance of asphalt mixtures. Although the mix with 60% SDA showed a lower tensile strength ratio (TSR), indicating high moisture susceptibility, than those prepared with OPC, the TSR value was still higher than the minimum requirement by the specification in state standard, which is 80%. On the other hand, Liew et al. [17] found that using SDA as a mineral filler is not beneficial for producing asphalt mixtures in terms of performance but helps with the economic and environmental burdens. Using the waste, SDA may considerably reduce the costs of asphalt concrete production [18]. Dimter et al. [19] found that the use of SDA can reduce the cost of asphalt concrete production by up to 15%. Although there are

proven benefits of using SDA in asphalt concrete, a few challenges are associated with its use. One of the main challenges is the variability of SDA properties, which directly affects the properties of the made asphalt mixture [3,14]. The variability includes the type of burned wood, the combustion conditions, and the collection method of the ash.

Overall, using SDA is feasible to improve the performance of asphalt pavements while reducing the economic and environmental burdens. However, the scope of existing research is still limited. Further research is needed to have more experimental data to confirm and fully understand the potential of SDA as a sustainable mineral filler and, meanwhile, to address the associated challenges. The novelty of this research lies in its comprehensive approach to analyzing the varied benefits and applications of SDA as a mineral filler in asphalt mixtures. It aimed to bridge the critical knowledge gap between waste material repurposing and infrastructural development, highlighting a pioneering direction for sustainable road construction.

2. Objectives and Scope

The current study aims to produce a sustainable asphalt mixture using SDA to substitute limestone dust (LD). An experimental investigation was conducted to evaluate asphalt mixtures containing different percentages of SDA ranging from 0% to 60% by weight of mineral filler. All the mixes had the optimal asphalt content, which was determined using the Marshall mix design method. Experimental tests were performed to evaluate the influence of SDA content on the engineering properties of asphalt concrete, which include Marshall properties, resilient modulus, moisture susceptibility, and rutting resistance. In addition, scanning electron microscopy (SEM) analysis was employed to examine the crystal structure of the limestone dust, sawdust, and SDA. The comprehensive study aims to provide an understanding of the mechanism and quantitative use of SDA on the performance improvement of the wearing course and, consequently, the sustainability of whole pavement structures. The flowchart in Figure 1 illustrates the methodology of the experimental work.

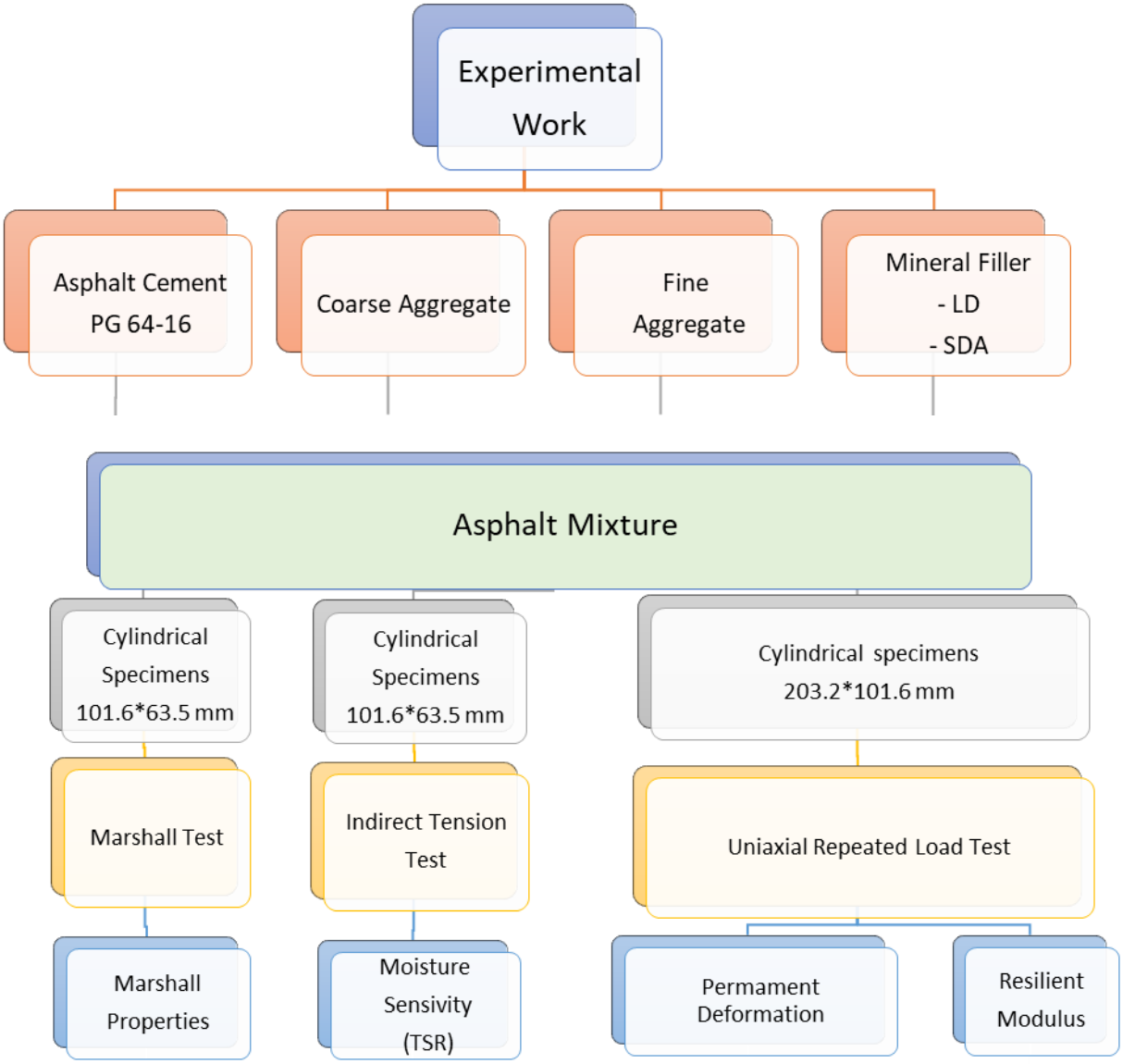

Figure 1: Flowchart of Experimental Work.

3. Material Section

3.1. Asphalt Cement

A performance grade (PG), PG 64-16, asphalt binder was used to prepare the asphalt mixtures. The physical properties of the asphalt binder were evaluated, and the results are shown in Table 1.

Table 1. Physical Properties of Asphalt Cement.

Asphalt cement	Properties	Temperature Measured °C	Measured Parameters	Specification Requirements, AASHTO M320-05
Original	Flash Point (°C)	-	298	230 °C, min
	Viscosity at 135 °C (Pa.s)	-	0.487	3 Pa.s, max
	DSR, G/sinδ at 10 rad/s (kPa)	58	3.3412	1.00 kPa, min
		64	2.1084	
		70	0.845	
RTFO Aged	Mass Loss (%)	-	0.633	1%, max
	DSR, G/sinδ at 10 rad/s (kPa)	58	4.1774	2.2 kPa, min
		64	3.1381	
		70	1.9084	
PAV Aged	DSR, G.sinδ at 10 rad/s (kPa)	28	4672	5000 kPa, max
		25	6398	
	BBR, Creep Stiffness (MPa)	-6	126.2	300 MPa, max

3.2. Aggregate

Crushed quartz aggregates with a nominal maximum size of 12.5 mm (1/2 inch) were used in this study. Table 2 lists the physical properties of the aggregates.

The proportioning of the coarse and fine aggregates was based on the gradation requirement for the Type III A mix, which is recommended for wearing courses by SCRB specification [20]. The gradation curve for the aggregate is shown in Figure 2.

Table 2. Physical Properties of Aggregates.

Property	ASTM Design	Test Outcomes	Specification of SCRB [20]
Coarse Aggregate			
Apparent Specific Gravity	C-127	2.638	-
Bulk Specific Gravity		2.631	-
Water Absorption, (%)		0.272	-
Soundness (Sodium Sulfate Solution Loss), %	C-88	3.9	12 max.
Percent Wear (Los Angeles abrasion), (%)	C-131	19	30 max.
Flat & Elongated (5:1), (%)	D4791	5	10 max.
Fractured Pieces, (%)	D5821	94	90 min.
Fine Aggregate			
Apparent Specific Gravity	C-128	2.619	-
Bulk Specific Gravity		2.557	-
Water Absorption, (%)		0.824	-
Clay Lump and Friable Particles, (%)	C-142	0.94	3 max.
Sand Equivalent (%)	D2419	56	45 min.

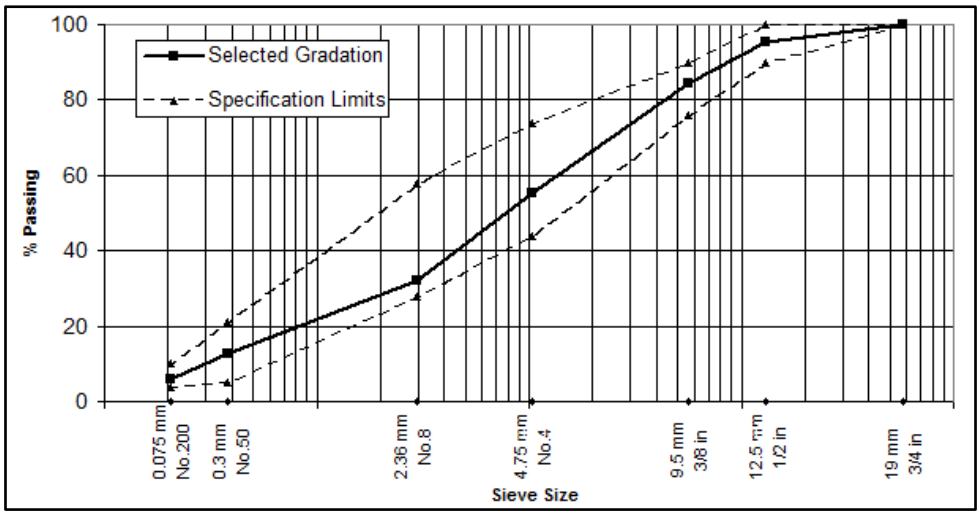

Figure 2. Selected gradation with SCRB specification limit.

3.3. Mineral Filler

Mineral filler is non-plastic particles passing sieve No. 200 (0.075mm). The present study used limestone dust (LD) as a conventional mineral filler. Table 3 shows the physical characteristics of the limestone dust.

Table 3. Physical Properties of Mineral Filler.

Properties	Results
Specific Gravity	2.73
Passing Sieve No.200, %	97

3.4. Saw Dust Ash

Sawdust (SD) was brought from the timber sawing workshops. The collected sawdust was burned in a wood-burning stove for approximately 2 hours at a temperature ranging from 400 ˚C to 450 ˚C; thereafter, the ash was left to cool down. The ash was then collected and sieved using the sieve No. 200 (0.075 mm). The portion that passes the sieve was used directly as a

filler, whereas those retained on the sieve were grounded properly to a finer size using a soil crusher machine and re-sieved. The chemical composition and physical properties of the SDA are given in Table 4. Figure 3 shows the states of the SD and the SDA.

Table 4. Chemical composition and physical properties of SDA.

CaO	SiO_2	Al_2O_3	MgO	Fe_2O_3	Na_2O	K_2O	P_2O_5	Specific gravity	% Passing sieve No. 200 (0.075 mm)
8.36	65.2	9.01	5.26	1.95	1.13	4.76	0.432	1.94	97

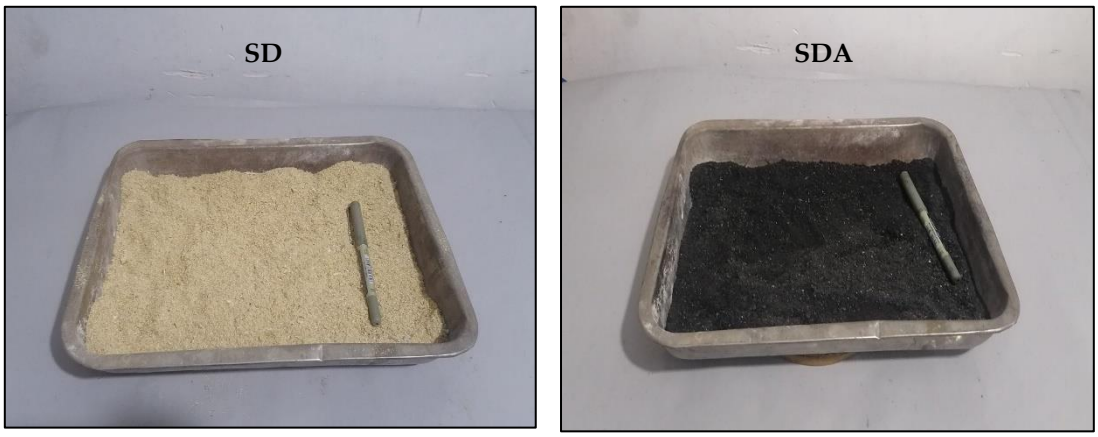

Figure 3. Powdered form of SD and SDA.

4. Experimental Work

4.1. Mix preparation

Initially, the aggregates were sieved by sieve sizes 19, 12.5, 9.5, 4.75, 2.36, 0.3, and 0.075 mm. The sieved aggregates were then batched as per the design aggregate gradation shown in Figure 2. The batched aggregates and the mineral fillers were then loaded in the mixing bowl and kept

in the oven for heating at 150˚C for 6 hours. Meanwhile, asphalt binder was also heated to a temperature ranging from 150-155˚C for 2 hours. After that, the preheated asphalt binder was added to the aggregates based on the weight calculated using the Marshall mix design method. The mixing of aggregates and the asphalt binder was performed for two minutes. To ensure uniform compaction temperature, the bowl with the mixed components was placed in the oven for 10 minutes at 140˚C. During this time, the 100˚C preheated compaction mold is prepared. The material was then loaded into the mold and compacted according to the requirements of the test type.

4.2. Testing methods

4.2.1. Scanning Electron Microscope (SEM)

SEM scans the surface of the material cross-section using a focused beam of electrons to examine the material structure at the microscopic scale, which can provide direct visual information about the surface topography, crystal structure, and material composition. In this study, SEM was employed to examine the 3D surface topography as well as the morphology of the crystals of limestone dust (LD), sawdust (SD), and sawdust ash (SDA).

4.2.2. Marshall Properties

The specimen for the Marshall test was made for all mixes in triplicate. Certain weights of mixes were loaded into the cylindrical molds and compacted on both sides by 75 blows on each side. The compaction level is equivalent to the pavement exposure to high traffic levels ($>10^6$ ESAL). After that, the samples within the molds were left to cool overnight and then de-molded and immersed in water for 30-45 minutes at a controlled temperature of 60℃ to evaluate Marshall test parameters, such as stability and flow (ASTM D6927). The Marshall stability is the highest load the specimen can withstand before failure; the Marshall flow is the total vertical plastic deformation of the specimen. The other measurements through the Marshall test are the

volumetric properties, including the percentage of air voids (%AV), the void content of mineral aggregate (%VMA), and the content of the voids filled by asphalt (%VFA).

4.2.3. Moisture Susceptibility

An indirect tensile test was carried out to assess the moisture susceptibility of the asphalt mixtures [21, 22]. In this test, a compressive load is applied at a rate of 50.8mm/min on the diametrical direction of the cylindrical specimens until the specimens split into two halves along the vertical diameter of the cross-section plane. The test was conducted on unconditioned and conditioned asphalt mixtures as per ASTM D 4867.

Six specimens (3 each for unconditioned and conditioned states) were prepared with an air void of 7±1% determined using a commonly followed trial-and-error approach. In this approach, trial samples were prepared with different compactive efforts, and the number of compaction blows corresponding to 7±1% air voids was adopted to prepare actual test samples used to evaluate moisture sensitivity. Unconditioned samples were tested under a normal temperature of 25°C without any conditioning process, whereas the other set of specimens (conditioned specimens) were subjected to a cycle of freeze and thaw exposed at temperature -18 ± 2°C for 16 hours and immediately another 24 hours at 60 ± 1°C. Following the conditioning process, the conditioned samples were taken out and tested at the normal temperature of 25°C.

The tensile strength was calculated according to Eq. (1) for unconditioned and conditioned specimens. Tensile strength ratio (TSR) was evaluated to understand the behaviour of the asphalt mixture against moisture damage. TSR is the ratio of the indirect tensile strength of the conditioned specimens (ITSc) and unconditioned specimens (ITS_d) as given in Eq. (2)

$$\mathbf{ITS} = \frac{\mathbf{2000 * P}}{\mathbf{\pi t D}} \quad (1)$$

$$\mathbf{TSR} = \frac{\mathbf{ITS}_c}{\mathbf{ITS}_d} \quad (2)$$

where P is the ultimate applied load (N), t is the thickness of specimen (mm), D is the diameter of the specimen (mm), TSR is Tensile Strength Ratio (%),

ITS_c is the Indirect Tensile Strength of the conditioned sample (kPa), and ITS_d is the Indirect Tensile Strength of the unconditioned sample (kPa)

4.2.4. Uniaxial Repeated Loading Test

The uniaxial repeated loading tests were conducted using the pneumatic repeated load system (PRLS). The cylindrical specimens of the size 101.6 mm (4 in) in diameter and 203.2 mm (8 in) in height were used for the test. These specimens were compacted through a double plunger technique, where a hydraulic compression machine applied a load of 65,000 lb (29,491 kg) on both sides of the test specimen for a time period of 1 minute. Two series of tests were conducted on these compacted test specimens. One was for the resilient modulus at a controlled temperature of 20°C (68°F), and another was for permanent deformation at 40°C (104°F). The repetitive compressive load was applied using the axial stress of 0.137 MPa (20 psi) in the form of a rectangular wave at a frequency of 1 Hz, with 0.1 seconds under loading followed by rest for 0.9 seconds. The resilient deflection was recorded at a time in the repetition range of 50~100, which was used to calculate the resilient modulus. The axial permanent deformation was recorded at a series of the number of loading repetitions. The permanent strain (ε_p) was calculated using the Eq. (3):

$$\varepsilon_p = \frac{p_d \times 10^6}{h} \quad (3)$$

Where ε_p is axial permanent strain, p_d is axial permanent deformation, and h is specimen height. The recorded permanent deformation against the number of load repetitions can be represented using the Eqn. (4), which was originally suggested by Monismith et al. [23] and Barksdale [24] and implemented by Abass et al. [25] and Albayati et al. [26].

$$\varepsilon_p = aN^b \quad (4)$$

Where N is the number of load repetitions, a and b are two constants.

The resilient strain, ε_r, and resilient modulus, Mr, were calculated using the Eqs. (5) and (6):

$$\varepsilon_r = \frac{r_d \times 10^6}{h} \quad (5)$$

$$M_r = \frac{\sigma}{\varepsilon_r} \quad (6)$$

Where r_d is axial resilient deflection, h is specimen height, and σ is axial stress.

5. Mix Design

Marshall method of mix design (ASTM D6927) was used for producing the asphalt mixtures. Optimum asphalt content (OAC) was determined by averaging the asphalt contents corresponding to the maximum stability and the maximum density. For each SDA content, five percentages of asphalt cement were used starting from 4.3% by the weight of the total mix with an increment rate of 0.3%. These are 4.3, 4.6, 4.9, 5.2, and 5.5%. The obtained OACs are presented in Table 5. It's important to highlight that when the SDA content was limited to 15%, there was no discernible change in the optimum asphalt content, likely due to the minimal quantity of SDA incorporated in the asphalt mixtures. Due to the rough surface of SDA particles and the high surface area compared to limestone dust particles, OAC increased slightly with the increase in SDA content. Along with the morphology of SDA, the increase in OAC is also attributed to the lower specific gravity of SDA (1.94) compared to limestone dust (2.73), leading to an increase in the volume of filler in the mixes prepared using SDA. The volume of filler increases with the increase in replacement percentage, thereby resulting in higher OAC for SDA mixes. In particular, the demand for asphalt cement increased linearly with a constant proportionality of 0.15%, with an increase in the SDA content by 30%. This implies that the required OAC for the production of asphalt mixtures with 60% SDA is higher than control mixes (0% SDA) by 3 kg for each ton of mix.

Table 5. OAC for mixes with various SDA content.

SDA Content, %	0	15	30	45	60
OAC, %	4.70	4.70	4.85	4.90	5.00

Table 6 presents the detailed ingredient breakdown for the asphalt concrete mixes with different SDA contents, considering the OAC and aggregate proportions.

Table 6. Ingredient breakdown for one metric ton (1000 kg).

SDA Content (%)	OAC (kg)	Coarse Aggregate (kg)	Fine Aggregate (kg)	Filler (kg)	
				LD	SDA
0	47	390.73	495.56	66.71	0
15	47	390.73	495.56	56.70	10.01
30	48.5	390.12	494.78	46.63	19.98
45	49	390.03	494.52	36.61	29.96
60	50	389.50	494.00	26.60	39.90

6. Results and Discussion

6.1. SEM Analysis

Figure 4 displays the external morphology (texture) and crystalline structure of the LD, SD, and SDA at a magnification level of 5 kX. Clearly, there is a difference between the morphology of the three categories of materials. The crystalline structure of the LD is obvious with rhombohedral or scalenohedral particle shape which belongs to the calcite crystals. Also, these crystals tend to agglomerate in the form of polycrystalline structures. Further inspection revealed the existence of crevices, ridges, and valleys on the particle surfaces, representing the irregular nature of the crystalline structure of limestone. The SEM for the SD typically shows a cellular structure that reflects the nature of the timber. Cells with fibers, vessels, and tracheid

shapes were clearly identified. The rounded shape of cells is apparently due to the hygroscopicity of the material. After burning the SD, the SDA looks vastly different under the SEM, as the combustion has destroyed the original cellular structures, leaving behind most mineral residues. Also, more crystalline or amorphous structures with flat lamellar, irregular, and fragmented particles were observed. Due to the release of volatile substances during the combustion process, the SEM for SDA reveals a certain level of surface porosity with a variety of pores, voids, and cavities, which imparts a rough surface texture to SDA.

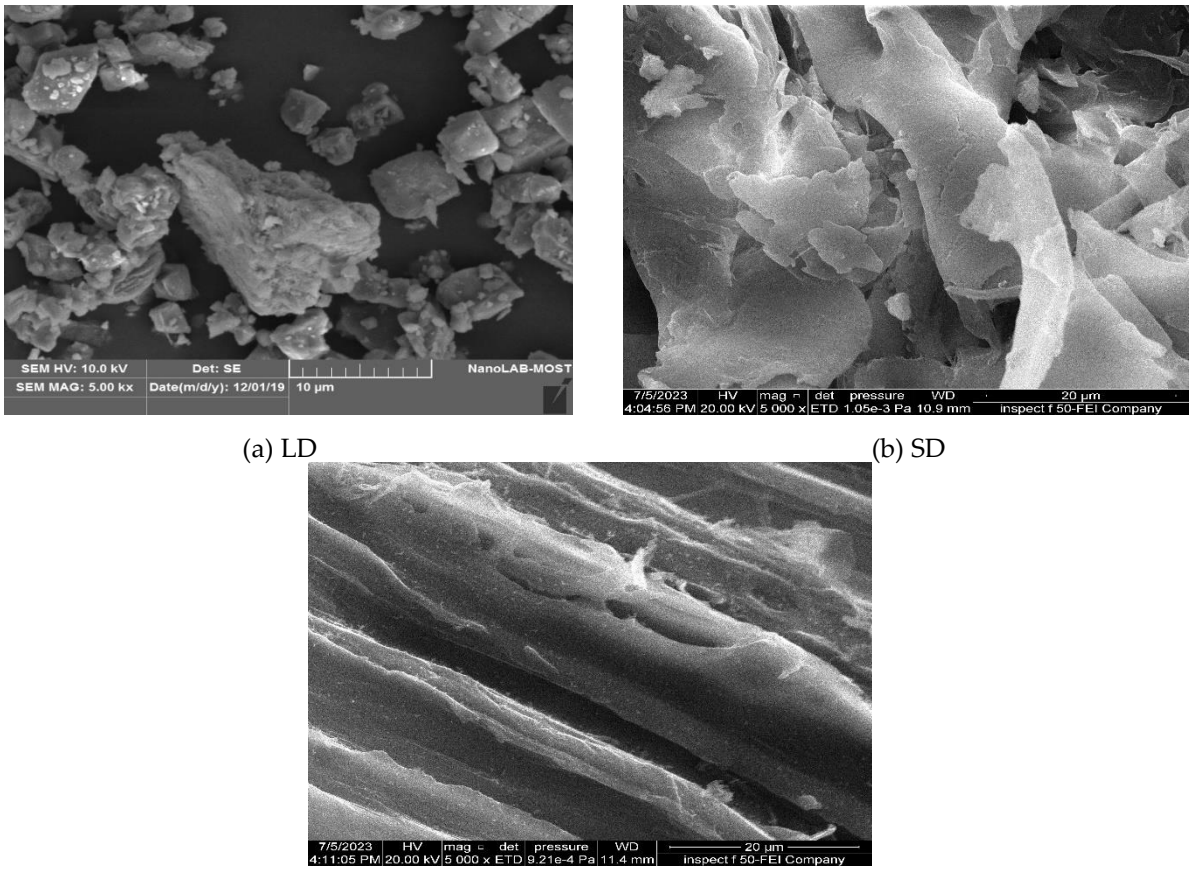

(a) LD (b) SD

(c) SDA

Figure 4. SEM Images of the LD, SD, and SDA.

6.2. Marshall and Volumetric Properties

Figure 5a shows the value of Marshall stability at different SDA content. As can be seen, there is an improvement in the stability as the SDA content increases. Compared to the control mix

(i.e., 0% SDA), the highest improvement corresponds to the mix prepared with 60% SDA content, i.e., 10.2%. This improvement in load resistance could be attributed to the ability of the pozzolanic material to increase the viscosity of asphalt binder, thereby increasing the binder's stiffness and load-carrying capacity. For SDA content <30%, the stability value increases by around 0.18 kN for each 15% increase in SDA content, whereas it shifts to approximately 0.35 kN when the SDA content increases from 30 to 60%.

The flow results (shown in Figure 5b) are in consensus with this fact: as the SDA content increases, the flow decreases. Although the replacement of 60% of limestone filler by SDA leads to the highest reduction in the flow value, the corresponding value of 3.04 mm is still within the specification limit (2 to 4 mm).

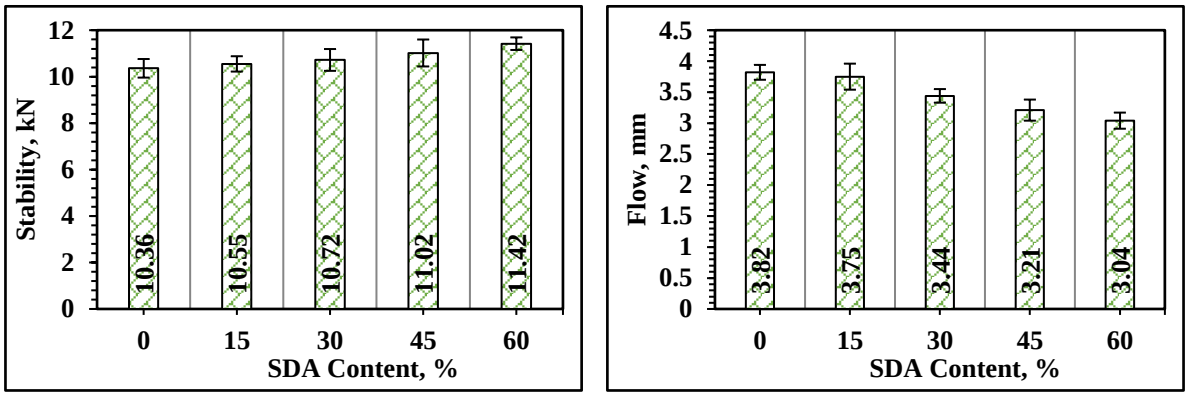

(a) (b)

Figure 5. Effect of SDA content on Marshall properties (a) Stability and (b) Flow.

As per the plot of mixture density versus SDA content presented in Figure 6, the bulk density shows a decreasing trend with the addition of SDA. This could be attributed to the lower density of SDA compared to the replaced LD mineral filler. With the increase in SDA content, there is an increase in the volume of filler in the mix, which eventually densifies the asphalt mixture.

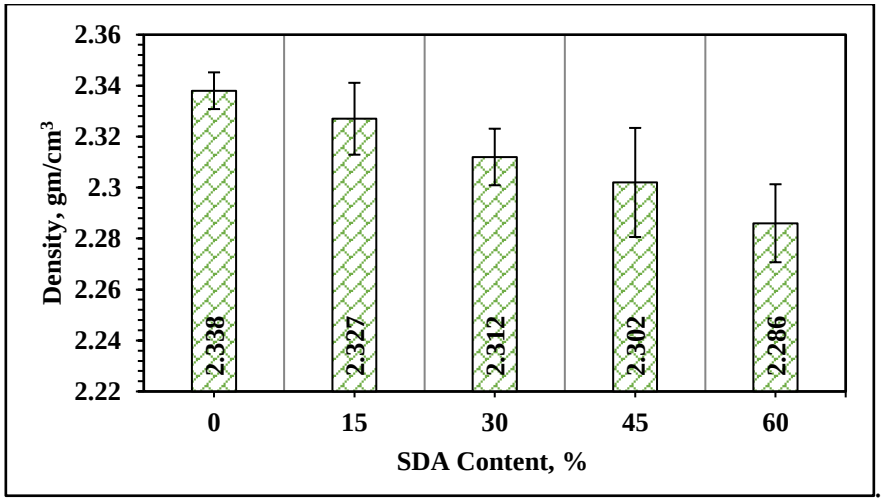

Figure 6. Effect of SDA content on bulk density.

In conjunction with the above, as demonstrated in Figure 7, the trend observed for the effect of SDA content on the air voids values (AV%) is opposite to that observed with density. The higher the SDA content, the higher the AV% due to the roughness of SDA particles, which restricts the sliding of aggregate particles among each other. Nevertheless, using SDA with any content investigated in this research resulted in mixtures that meet the air voids requirement between 3 and 5 percent. This finding aligns with those obtained by Osuya and Mohammed [13] and Karati et al. [14].

The voids in mineral aggregate (VMA) are essential volumetric properties that demonstrate the volume of the intergranular void space between the aggregate particles and provide a measure of compaction efficiency. As depicted in Figure 8, with the increase in SDA content, the VMA increases. The primary reason is that SDA particles are often smaller and less dense than LD, creating more void spaces in the aggregate skeleton and manifesting the need for further compaction. Additionally, the absorption of asphalt binder due to the pronounced porosity of SDA may also contribute to higher VMA values. Compared to 0% SDA, the VMA of a mix with 60% SDA increased by 6.5%.

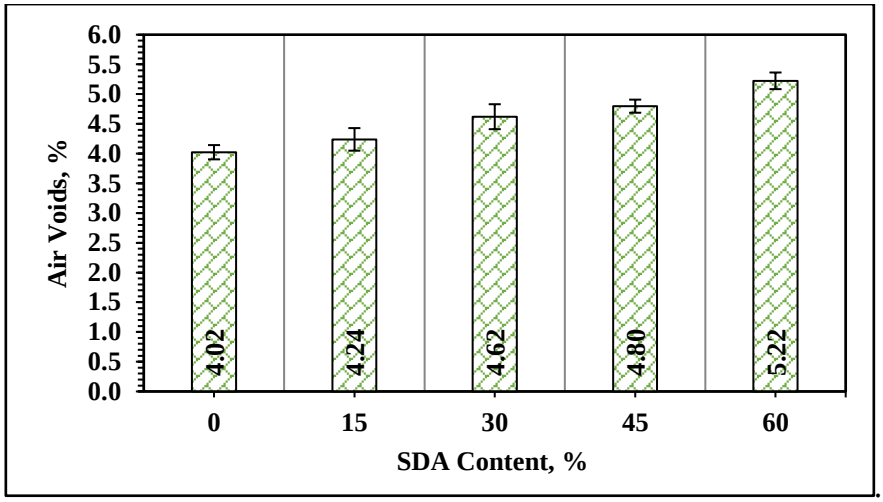

Figure 7. Effect of SDA content on air voids.

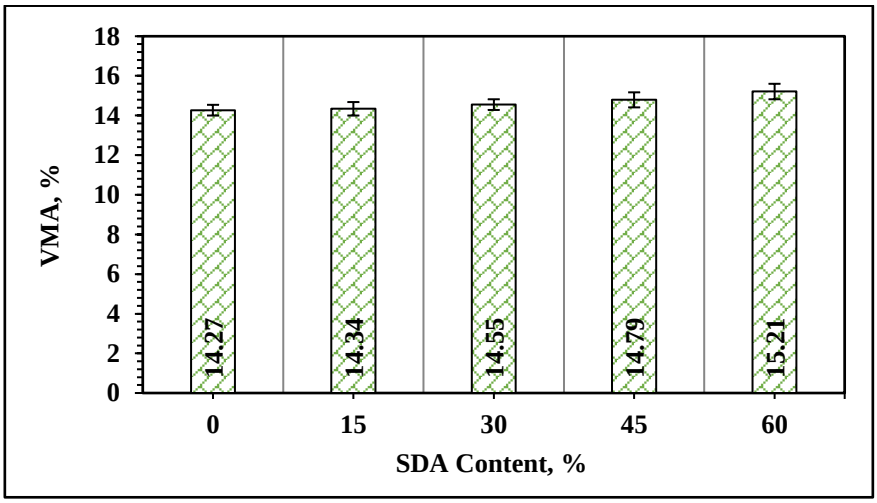

Figure 8. Effect of SDA content on voids in mineral aggregate.

6.3. Effect of SDA on Moisture Susceptibility:

The splitting tensile strength of the conditioned and unconditioned specimens is presented in Figure 9a. One of the most notable findings was that all SDA mixes led to higher ITS in dry conditions. When compared to the control mix, the ITS_d value of the mixes modified with 15%, 30%, 45%, and 60% SDA was increased by 1.5%, 2.4%, 3.8%, and 4.3%, respectively. This improvement in tensile strength is mostly due to the rough surface of SDA particles, which creates an effective bond with asphalt binder. On the other hand, the use of SDA up to 45%

resulted in a remarkable rise in ITSc, but a further increase in SDA content showed a low ITSc value.

Based on the TSR results exhibited in Figure 9b, it can be observed that the mixes modified with SDA have a slightly higher TSR value than the control mix, reflecting higher resistance to moisture susceptibility. The trend of TSR stays constant for the SDA contents of 15 and 30%. Interestingly, with an extra 15 percent (i.e., 45% SDA content), the TSR reaches the peak value of 87 %. Further increase in SDA content resulted in a decrease in TSR value. This may be attributed to the high air voids at higher SDA content in the mix. These voids might retain moisture during the conditioning of the specimen. Due to the freezing of moisture in these air pockets coupled with the size expansion for the ice lenses followed by thawing under a temperature of 60˚C, some weak points developed in the aggregate skeleton, which caused a reduction in tensile strength. Nevertheless, the TSR values for all the asphalt mixtures prepared using SDA were above the minimum threshold (TSR ≥ 80%) recommended for a moisture-resistant asphalt mixture.

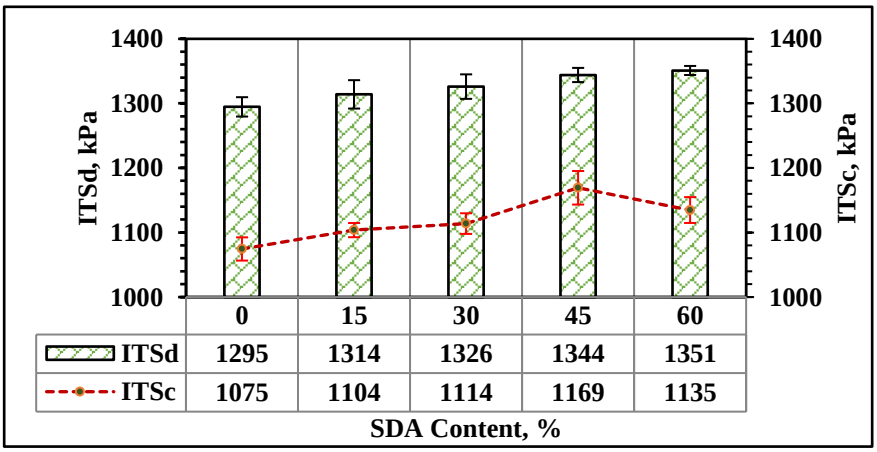

(a)

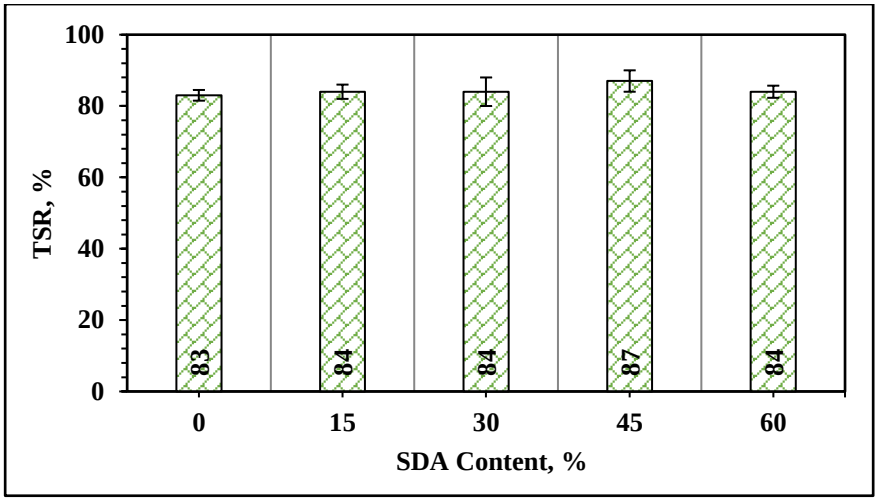

(b)

Figure 9. Effect of SDA content on Moisture Susceptibility (a) ITS and (b) TSR.

6.4. Effect of SDA on Resilient Modulus

Figure 10 depicts the elastic property of the mixes as defined by the resilient modulus (Mr). It can be seen that there is a slight improvement in Mr value with the application of SDA. When the SDA content increases, the Mr also increases. The highest improvement was achieved with the use of 60% SDA. The corresponding improvement rate was 3% compared to the control mix. The improvement in Mr values could be attributed to the improved cohesion properties of asphalt binders, which is due to the stiffening effect of SDA.

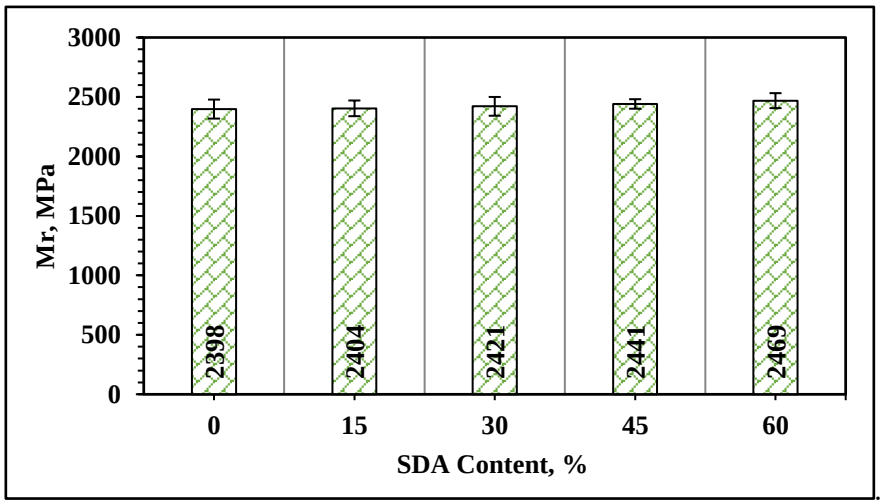

Figure 10. Effect of SDA content on Mr.

6.5. Effect of SDA on Permanent Deformation

Figure 11 shows the results of the permanent deformation test in terms of permanent strain and the number of load applications (N) for different SDA contents. Log scales are employed to display the relationship in the form of a straight line, on which the SDA effect can be characterized in terms of the intercept (a) and slope (b). The intercept represents the permanent strain at N = 1, and the slope represents the accumulation rate of permanent strain through N load applications. Together, these two coefficients can describe the ability of asphalt concrete specimens to withstand permanent deformation. The lower the two values, the higher the rutting resistance of the mix. As shown in Figure 11, it was very hard to differentiate the asphalt mixtures through the graphical presentation, which caused the effect of SDA to be invalidated. Therefore, it was decided to examine the data in terms of the permanent deformation coefficients as well as the permanent strain at the 1000th load repetition. This combines the effects of intercept as well as slope. The intercept data presented in Table 6 showed that SDA content negatively affects the rutting resistance. This behavior could be attributed to the high air voids in the asphalt mixtures prepared with the use of SDA. Therefore, these mixes are more prone to further densification, leading to higher permanent microstrain at the first load repetition during the test.

In contrast to intercept results, the slope results indicate that SDA addition, in general, improves the rutting resistance of asphalt concrete. In comparison to the control mix, the use of 60% SDA resulted in lowering the slope value by 16.9 percent. To ascertain the role of SDA content on the permanent deformation of asphalt concrete, in view of the contradictory results of intercept and slope, the permanent strain endured at 10,000 load repetitions was noted (as shown in the last column of Table 7). The value of microstrain at 10,000 load repetitions implied that the use of SDA improves the rutting resistance. In comparison with the control mixes of 0% SDA

content, the value of permanent microstrain was found to be lower for the mixes of 15%, 30%, 45%, and 60% SDA content by a percentage of 1.23, 2.25, 8.70, and 12.08, respectively, The above results indicate the positive role of the SDA in producing a high stiffness asphalt concrete with better stone-stone contact which consequently reduces the possibility of the high-temperature rutting.

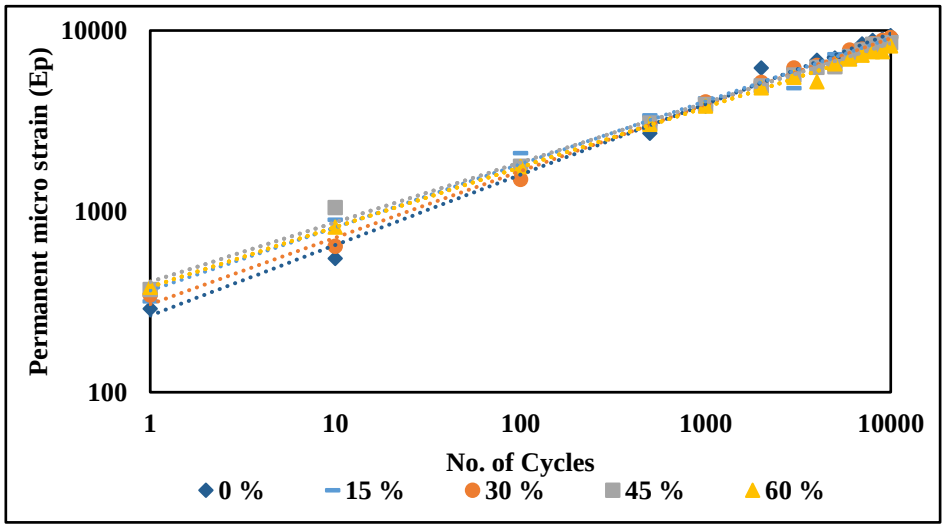

Figure 11. Effect of SDA content on the relation of permanent deformation vs. load repetition.

Table 7. Effect of SDA content on the permanent deformation parameters.

SDA content, %	40°C		
	a	b	(ε_p) at N = 10,000
0	290	0.378	9370
15	318	0.366	9254
30	345	0.356	9158
45	370	0.341	8554
60	380	0.334	8237

7. Cost Analysis

Table 8 provides the reference price for the materials used in this study. The total cost per cubic meter for each mix, based on these referred price, and the corresponding percentage decrease in cost compared to the control mix (0% SDA) are shown in Figure 12.

Table 8. Reference prices for mix constituents.

Material	**Cost***
Coarse aggregate	11$/Ton
Fine aggregate	8.16$/ Ton
Mineral filler	60$/ Ton
Asphalt cement	270$/ Ton
SDA	30$/ Ton

* The cost of materials is sourced from the Ministry of Industry and Minerals in Iraq.

The cost analysis shows that the cost of producing asphalt mixtures was reduced by incorporating SDA. The cost reduction aligns with the increase in SDA content, though the rate of decrease varies. For example, the cost for mixes with 15% SDA content shows a modest decrease of 1.56%, while mixes with 60% SDA content exhibit a more substantial decrease of 3.78%.

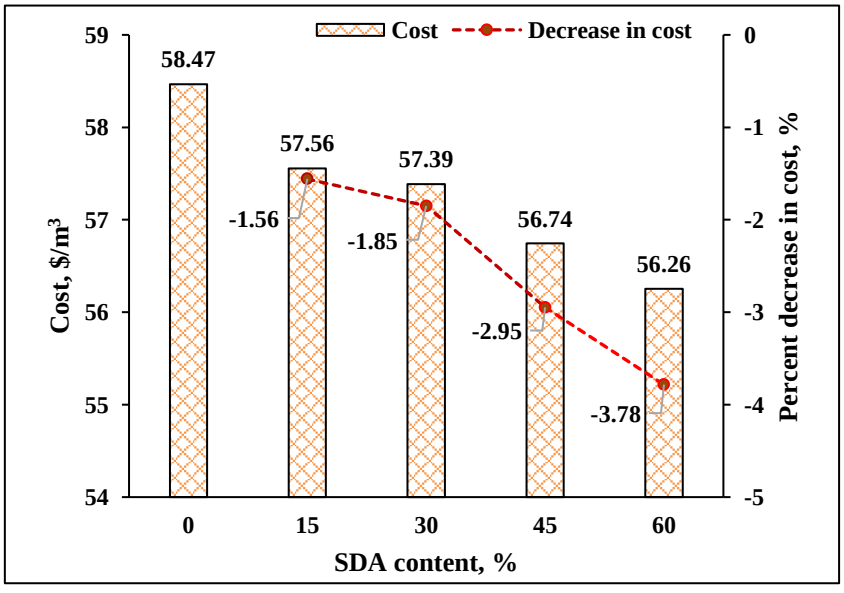

Figure 12. Cost per cubic meter and percentage decrease in cost.

To evaluate the economic efficiency and determine the optimal SDA content that maximizes performance at minimal cost, this study utilizes a "Gain" index. This index is a comparative ratio that assesses the rate of change in key properties of the modified mixtures compared to the control mix (CM) against the rate of change in mixture cost. Specifically, the numerator represents the property value for a given mix divided by the value for the control mix, and the denominator represents the cost for the given mix divided by the cost of the control mix. A higher gain index value indicates better performance at a lower cost. Figure 13 presents the gain values for various mechanical properties of asphalt mixes modified with different dosages of SDA. The mechanical properties considered include Stability, TSR, Mr, and εp (permanent deformation). The gain values provide a comprehensive assessment of each mix's effectiveness. The gain values were analyzed across all mechanical properties to identify the optimal SDA dosage. The total gain values obtained were 4.10, 4.15, 4.35, and 4.44 for mixes with 15%, 30%, 45%, and 60% SDA, respectively. The mix with 60% SDA demonstrated the highest gain sum, indicating it is the optimal choice for enhancing asphalt mixture performance while maintaining economic efficiency.

Furthermore, compared to the control mix (0% SDA), the mix with 60% SDA shows notable improvements in key properties: Stability improved by 10.23%, TSR by 1.2%, Mr by 2.9%, and permanent deformation resistance by 12.09%. Based on the results, 60% SDA is recommended as the optimal dosage, offering significant improvements in pavement performance and providing an efficient and economical solution for the production of the asphalt mixture.

However, further research and efforts for practical application are essential to realize the potential of SDA to promote sustainable practices in the pavement engineering industry.

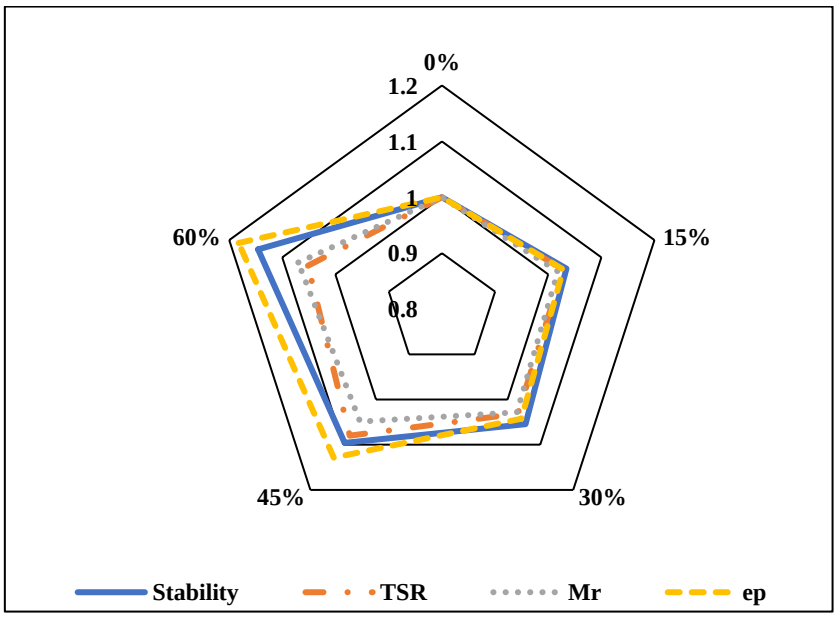

Figure 13. Gain values for different asphalt mixtures.

8. Conclusions

While numerous waste materials pose environmental challenges, they can be effectively repurposed in asphalt concrete to enhance the material properties and the sustainability of the industry. The key objective of the present study is to investigate the potential of sawdust ash (SDA) as an alternative to traditional limestone dust, which is used as a mineral filler in asphalt concrete. Limestone dust was replaced with SDA at different proportions (0%, 15%, 30%, 45%, and 60% by weight of mineral filler). Marshall method was adopted for mix design, and the performance of asphalt mixtures, including moisture susceptibility, resilient modulus, and permanent deformation, was evaluated. The following conclusions can be drawn based on the study:

1. SEM images showed LD has a rhombohedral or scalenohedral structure, while SDA displays a combination of crystalline and amorphous structures, with flat and broken particles featuring a rough surface texture.
2. A positive correlation exists between the Marshall stability and the SDA content. The stability improves more significantly when SDA content increases from 30% to 60% than from 0% to 30%.
3. The bulk density of mixes shows a decreasing trend with the increase in SDA content. The trend was the opposite for volumetric properties (AV and VMA). Compared to 0% SDA, the VMA of mixes with 60% SDA was higher by 6.5 percent.
4. All the asphalt mixtures examined in this study had TSR values greater than 80%, suggesting the efficiency of SDA against moisture susceptibility. The peak value of TSR, i.e., 87%, was observed using 45% SDA.
5. The Mr value improved slightly as the SDA content increased. The highest improvement was observed with the use of 60% SDA. In comparison with the control mix, the corresponding improvement rate was found to be 3 percent.
6. By the slope of the linear relationship between the permanent strain and the number of cycles (when used in log scale), the mixes with 60% SDA exhibited improved rutting resistance. However, by the intercept value, the control mix (with 0% SDA) exhibits the lowest initial permanent strain. Overall, when both parameters were considered together, the mix of 60% SDA shows the best on rutting resistance.
7. Incorporating 60% SDA resulted in the highest gain value, representing an optimal solution for producing a cost-effective and sustainable asphalt pavement. Beyond 60% SDA, there may be a likelihood of moisture-induced damage in the asphalt pavement, as evident from the TSR value, which is highest for 45% SDA mixes.

In summary, this study concludes that substituting 60% of traditional mineral filler (limestone dust) with the SDA has improved performance for the modified asphalt concrete regarding rutting resistance, moisture susceptibility, resilient modulus, and stability. As can be observed from the results of the present study, the variation in the performance of 45% SDA mixes and 60% SDA mixes was quite minimal. Thus, the scope of the present study was limited to 60% SDA replacement. However, the results may alter when different aggregates and asphalt binder sources are used. Hence, it is suggested to incorporate other sources of mix components for validating the trend of the results obtained in the current study and thereby comment on the effectiveness of SDA with a wider research scope. While this study primarily focuses on performance characteristics and cost analysis, there is also a need for a comprehensive assessment that includes environmental impacts and life cycle costs.

References

1. Sukhija, M., Prasad, A. N., Saboo, N., & Mashaan, N. (2023). Assessment of virgin binder-blended rejuvenators and antistripping agents for hot recycled asphalt mixture. International Journal of Pavement Research and Technology, 16(5), 1226-1240.
2. Dimulescu, Catalina, and Adrian Burlacu. "Industrial Waste Materials as Alternative Fillers in Asphalt Mixtures." *Sustainability* 13.14 (2021): 8068.
3. Choudhary, J., Kumar, B., & Gupta, A. (2020). Utilization of solid waste materials as alternative fillers in asphalt mixes: A review. Construction and Building Materials, 234, 117271.

4. Mondal, Abhijit, R. N. G. D. Ransinchung, and Jayvant Choudhary. "Sustainable recycling of industrial waste fillers and reclaimed asphalt pavement to produce environmentally feasible warm mix asphalt." *Innovative Infrastructure Solutions* 8.1 (2023): 34. https://doi.org/10.1007/s41062-022-01006-4
5. Chaudhary, M., Saboo, N., Gupta, A., Hofko, B., & Steineder, M. (2020). Assessing the effect of fillers on LVE properties of asphalt mastics at intermediate temperatures. Materials and Structures, 53(4), 96.
6. Wang, Jie, Meng Guo, and Yiqiu Tan. "Study on application of cement substituting mineral fillers in asphalt mixture." International Journal of Transportation Science and Technology 7.3 (2018): 189-198. https://doi.org/10.1016/j.ijtst.2018.06.002
7. Choudhary, J., Kumar, B., & Gupta, A. (2020). Feasible utilization of waste limestone sludge as filler in bituminous concrete. Construction and Building Materials, 239, 117781.
8. Fan, Zhenyang, et al. "Effects of cement–mineral filler on asphalt mixture performance under different aging procedures." Applied Sciences 9.18 (2019): 3785. https://doi.org/10.3390/app9183785
9. Diab, Aboelkasim, and Mahmoud Enieb. "Investigating influence of mineral filler at asphalt mixture and mastic scales." International Journal of Pavement Research and Technology 11.3 (2018): 213-224. https://doi.org/10.1016/j.ijprt.2017.10.008
10. Choudhary, J., Sukhija, M., & Gupta, A. (2022). A comparative analysis of engineering and economical suitability of bituminous mastics containing waste fillers. Case Studies in Construction Materials, 17, e01640.

11. Choudhary, J., Asthana, G., Sukhija, M., Wagh, V. P., & Gupta, C. (2023, July). Effective utilisation of waste cement concrete dust in bituminous concrete. In Proceedings of the Institution of Civil Engineers-Transport (pp. 1-13). Emerald Publishing Limited.
12. Adegoke, Kayode Adesina, et al. "Sawdust-biomass based materials for sequestration of organic/inorganic pollutants and potential for engineering applications." Current Research in Green and Sustainable Chemistry (2022): 100274.
13. Osuya, D. O., and H. Mohammed. "Evaluation of sawdust ash as a partial replacement for mineral filler in asphaltic concrete." Ife Journal of Science 19.2 (2017): 431-440. https://doi.org/10.4314/ijs.v19i2.23
14. Karati, Sukanta, and Tapash Kumar Roy. "Effect of saw dust ash (SDA) and recycled asphalt pavement (RAP) in the bituminous concrete." E3S Web of Conferences. Vol. 368. EDP Sciences, (2023). https://doi.org/10.1051/e3sconf/202336802033
15. Fayissa, Basha, Oluma Gudina, and Biruk Yigezu. "Application of Sawdust Ash as Filler Material in Asphaltic Concrete Production." Civil and Environmental Engineering 16.2 (2020): 351-359. https://doi.org/10.2478/cee-2020-0035
16. Abbas, H., Al-Rubaee, R. H., & Baqir, H. H. (2023, July). Effect of sawdust ash as mineral filler on the properties of hot asphalt mixture. In AIP Conference Proceedings (Vol. 2775, No. 1). AIP Publishing.
17. Liew, S. I. N., Ng, C. M., Jaya, R. P., Hasan, M., Masri, K. A., Jaafar, Z. F. M., ... & Mashros, N. (2023, May). Influence of Sawdust Ash as filler in asphalt mixture. In AIP Conference Proceedings (Vol. 2688, No. 1). AIP Publishing.

18. Oba, Kenneth Miebaka, Tamunoemi Alu Long John, and Kaniyeh Anthony Ijeje. "Suitability of saw dust ash and quarry dust as mineral fillers in asphalt concrete." International Journal Of Engineering And Management Research 12.2 (2022): 24-29. https://doi.org/10.31033/ijemr.12.2.4
19. Dimter, Sanja, et al. "Laboratory evaluation of the properties of asphalt mixture with wood ash filler." Materials 14.3 (2021): 575. https://doi.org/10.3390/ma14030575
20. SCRB/R9. "General Specification for Roads and Bridges, Section R/9, Hot-Mix Asphalt Concrete Pavement, Revised Edition." State Corporation of Roads and Bridges, Ministry of Housing and Construction, Republic of Iraq (2003).
21. Albayati, Amjad H. "Mechanistic evaluation of lime-modified asphalt concrete." 7th RILEM International Conference on Cracking in Pavements: Mechanisms, Modeling, Testing, Detection and Prevention Case Histories. Dordrecht: Springer Netherlands, (2012). https://doi.org/10.1007/978-94-007-4566-7_89
22. Sukhija, M., Saboo, N., & Pani, A. (2023). Effect of warm mix asphalt (WMA) technologies on the moisture resistance of asphalt mixtures. Construction and Building Materials, 369, 130589.
23. Monismith, Carl L., N. Ogawa, and C. R. Freeme. "Permanent deformation characteristics of subgrade soils due to repeated loading." Transportation research record 537 (1975).
24. Barksdale, Richard D. "Laboratory evaluation of rutting in base course materials." Presented at the Third International Conference on the Structural Design of Asphalt Pavements,

Grosvenor House, Park Lane, London, England, Sept. 11-15, 1972. Vol. 1. No. Proceeding. 1972.

25. Abass, Bedour J., and Amjad H. Albayati. "Influence of recycled concrete aggregate treatment methods on performance of sustainable warm mix asphalt." Cogent Engineering 7.1 (2020): 1718822. https://doi.org/10.1080/23311916.2020.1718822
26. Albayati, Amjad H., and Harith Abdulsattar. "Performance evaluation of asphalt concrete mixes under varying replacement percentages of natural sand." Results in Engineering 7 (2020): 100131. https://doi.org/10.1016/j.rineng.2020.100131